

COVER SHEET

Paper Number: **2911**

Title: **Delamination Detection Using Guided Wave Phased Arrays**

Authors: Zhenhua Tian
Lingyu Yu
Cara Leckey

ABSTRACT

This paper presents a method for detecting multiple delaminations in composite laminates using non-contact phased arrays. The phased arrays are implemented with a non-contact scanning laser Doppler vibrometer (SLDV). The array imaging algorithm is performed in the frequency domain where both the guided wave dispersion effect and direction dependent wave properties are considered. By using the non-contact SLDV array with a frequency domain imaging algorithm, an intensity image of the composite plate can be generated for delamination detection. For the proof of concept, a laboratory test is performed using a non-contact phased array to detect two delaminations (created through quasi-static impact test) at different locations in a composite plate. Using the non-contact phased array and frequency domain imaging, the two impact-induced delaminations are successfully detected. This study shows that the non-contact phased array method is a potentially effective method for rapid delamination inspection in large composite structures.

INTRODUCTION

Advanced composite materials are contributing to a revolution in aerospace, marine and automotive applications. Unexpected damage can occur in composites due to impact events or material stress during off-nominal loading events. In particular, laminated composites are susceptible to delamination damage due to weak transverse tensile and interlaminar shear strengths. Delamination damage can occur largely internally to the composite such that a damage indication is barely visible to the naked eye on the composite surface. Such hidden delamination damage must be detected and evaluated before it becomes critical. Developments of rapid inspection techniques for detecting and quantifying damage in large composites are critical for ensuring operability and safety of composite structures.

For rapid damage inspection, an ultrasonic based image of the structure often gives output that quickly identifies and locates defects. Among various imaging methods,

Zhenhua Tian, Mechanical Engineering, University of South Carolina, Columbia, SC, 29208
Lingyu Yu, Mechanical Engineering, University of South Carolina, Columbia, SC, 29208
Cara Leckey, Nondestructive Evaluation Sciences Branch, NASA Langley Research Center,
Hampton VA, 23681

the guided wave phased array imaging is attractive since it uses sensors that are placed closed to each other in a compact format, steers the outputs of all sensors in a desired direction, and scans the entire structure like a radar [1], allowing for large area inspection with limited access. Intensive study has been conducted on the guided wave phased array beamforming and damage detection on metallic plate-like structures [1-3]. Some researchers have started investigating the use of phased arrays for anisotropic composite materials [4-8]. It has been found that the guided wave complexity caused by anisotropic and inhomogeneous properties in composite materials makes the traditional metal-based methods inappropriate and sometimes even misleading [9-11].

This paper presents a non-contact guided wave phased array method for detecting multiple impact induced delaminations in composite laminates. The phased array imaging technique is performed in frequency domain where both the guided wave dispersion effect and direction dependent wave properties are considered. Moreover, the phased array method is implemented with a non-contact scanning laser Doppler vibrometer (SLDV). Using measurements recorded at a small number of SLDV scanning points, for example 10×10 points in a rectangular grid array, the phased array method can generate an intensity image of the structure that identifies the damage location. For the proof of concept study, laboratory tests are performed using rectangular grid array scanning points from the non-contact SLDV. The tests are performed on a plate with two sites of impact induced delaminations at different locations. The results show that the two delamination sites can be successfully detected using the non-contact SLDV array. The remainder of this paper is organized as follows: Section 2 presents the formulation of phased array imaging in anisotropic composite plates; Section 3 presents the implementation of phased arrays by using a non-contact SLDV for detecting two delamination sites caused by impacts at different locations; Section 4 concludes the paper with discussion of results and planned future work.

PHASED ARRAY IMAGING ALGORITHMS

This section presents the algorithms for phased array imaging in anisotropic composites using an SLDV. Figure 1 gives the SLDV sensing layout for the phased array method. Guided waves are excited by a surface bonded piezoelectric wafer (PZT) actuator centered at the coordinate origin. A non-contact SLDV is used to take measurements in a small scanning area centered at the origin. The SLDV can measure velocities of guided waves via the Doppler Effect. Through the point-by-point measurement of guided waves at multiple scanning points on a predefined scan grid, the SLDV acquires a velocity wavefield $v(t, \mathbf{x})$ of guided wave propagation as a function of both time t and space \mathbf{x} [12-15].

With the data acquired over the SLDV scan region, the phased array data set is then constructed using selected SLDV scan points. Note that data collected at points within the scanned area can then be down-selected to construct arrays (e.g. those shown in the callout in Figure 1), giving the flexibility for constructing arrays of various configurations with only one SLDV scan. Assume the array points are at locations $\{\mathbf{p}_m\}$ ($m=0, 1, 2, \dots, M-1$), whose phase center satisfies $\frac{1}{M} \sum_{m=0}^{M-1} \mathbf{p}_m = \mathbf{0}$ (note the phase delay at the phase center is always zero). From the time-space

wavefield $v(t, \mathbf{x})$ acquired by the SLDV, the signal at the m^{th} array point (\mathbf{p}_m) can be denoted as $v_m(t)=v(t, \mathbf{p}_m)$. Its frequency spectrum can be

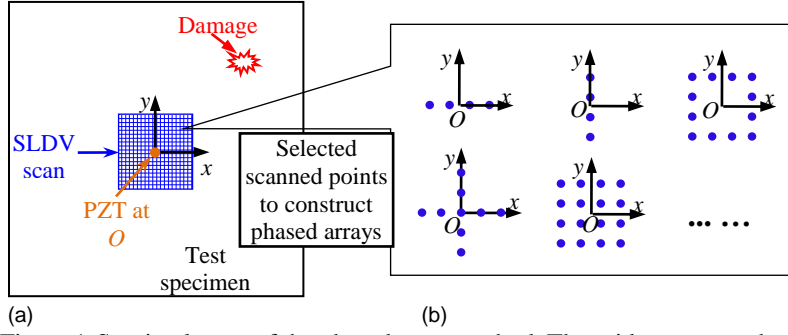


Figure 1 Sensing layout of the phased array method. The grid represents the scanning area of the SLDV. Any points within the scanned area can then be selected to construct phased arrays of various configurations, as shown in the diagram on the right side (blue dots illustrate possible selection of measurement points to construct phased arrays with different configurations).

derived using the Fourier transform, as:

$$V_m(f) = F [v_m(t)] = \int_{-\infty}^{\infty} v_m(t) e^{-j2\pi ft} dt \quad (1)$$

Using the frequency spectrum $V_m(f)$ of each array element, we can derive a synthesized frequency-space representation $Z(f, \mathbf{x})$ of the array[16]:

$$Z(f, \mathbf{x}) = \sum_{m=0}^{M-1} w_m V_m(f) e^{j[-\varphi(f, \mathbf{x}) - \Delta_m(f, \mathbf{x})]} \quad (2)$$

where,

$$\Delta_m(f, \mathbf{x}) = \mathbf{k}(f, \gamma) \cdot \mathbf{p}_m, \text{ and } \varphi(f, \mathbf{x}) = -2\mathbf{k}(f, \gamma) \cdot \mathbf{x} \quad (3)$$

$\Delta_m(f, \mathbf{x})$ is the phase delay applied to the m^{th} array point for beamsteering, and $\varphi(f, \mathbf{x})$ represents the spatial phase shift. As guided waves travel from the PZT to the damage and then back to the array, they undergo a spatial phase shift $\varphi(f, \mathbf{x})$. Thus, $-\varphi(f, \mathbf{x})$ is applied in Eq. (2) in order to compensate for the spatial phase shift. $\mathbf{k}(f, \gamma)$ is the wavenumber vector at the frequency f and wavenumber angle γ , and is obtained from wavenumber dispersion curves. γ is the wavenumber angle determined from the geometry relation as $\gamma = \theta + \beta$, where θ is the energy propagation angle and equals the angle of vector \mathbf{x} , i.e., $\theta = \angle \mathbf{x}$, and β is the skew angle corresponding to the energy propagation angle θ . The energy propagation angle and skew angle can be obtained from slowness curves. Weighting factors w_m can be used to further control the quality of the beamforming such as the beam shape. In this study, weighting factors are set equal to one.

Using the inverse Fourier transform, the frequency-space representation $Z(f, \mathbf{x})$ can be transformed back to the time-space domain, as:

$$z(t, \mathbf{x}) = F^{-1} [Z(f, \mathbf{x})] = \int_{-\infty}^{\infty} Z(f, \mathbf{x}) e^{j2\pi ft} df \quad (4)$$

where $z(t, \mathbf{x})$ is a synthesized time-space wavefield that represents the array beamforming in time-space domain. An inspection image of the plate to detect/locate

any existing damage is then acquired by building an intensity image with the pixel value at the location \mathbf{x} defined as:

$$I(\mathbf{x}) = |z(t = 0, \mathbf{x})|^2 \quad (5)$$

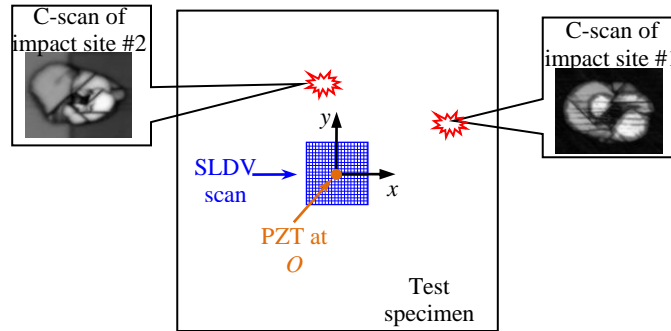


Figure 2 Sensing layout for impact-induced delamination damage detection. There are two delamination sites at (88, 39) mm and (-11, 75) mm. The grid represents the scanning area of the SLDV.

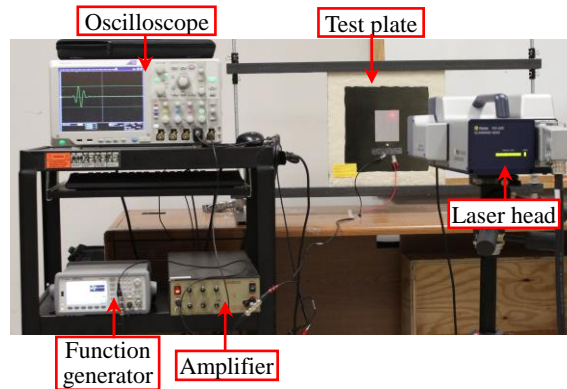


Figure 3 The experimental setup for impact-induced delamination damage detection.

DETECTION OF MULTIPLE DELAMINATIONS

The phased array method presented in the above section is used to detect delamination damage in a carbon fiber reinforced polymer (CFRP) composite plate with two delamination sites created by impacts at different locations. The test specimen is a 26 ply IM7/8552 composite laminate with a layup of $[(0_2/45_2/-45_2)_2/90]_S$ and dimensions of 381 mm \times 381 mm \times 2.8 mm, fabricated at NASA Langley Research Center (LaRC). The delaminations are created using a quasi-static indentation technique, which has been shown by other researchers to be an ideal method for controlled growth of impact-induced damage in composite laminates [17]. After the indentation test, an ultrasonic C-scan was conducted to confirm the existence of delamination damage in the plate. The resulting C-scan image in Figure 2 shows two delamination sites at coordinates of (88, 39) mm and (-11, 75) mm, respectively. The delamination at site #1 is approximately 1.03 inches by 0.83 inches and at site #2 is approximately 1.27 inches by 0.89 inches in size.

Figure 3 shows the overall experimental setup. A PZT wafer (APC 851: 7 mm diameter, 0.2 mm thickness) is bonded at the coordinate origin on the plate (as shown in Figure 2) to generate guided waves. The PZT excitation is a 3-cycle tone burst with

a frequency of 120 kHz generated by a function generator (model: Agilent 33522B) and then amplified to 40V by a power amplifier (model: Krohn-Hite 1506). An SLDV (model: Polytec PSV-400-M2) is used to acquire velocity wavefields of guided waves. The SLDV scan records data at 351×351 points with a spatial interval of 0.1 mm over a $35 \text{ mm} \times 35 \text{ mm}$ area. In the test, the laser beam is set normal to the plate such that the out-of-plane velocity is acquired.

Snapshots of the measured wavefield are plotted in Figure 4. At $25 \mu\text{s}$, Figure 4a shows incident A0 waves generated from the PZT wafer. At $110 \mu\text{s}$, Figure 4b shows the A0 waves reflected by the delamination damage of site #2 propagating in the direction close to -90 deg . At $120 \mu\text{s}$, in Figure 4c, and at $130 \mu\text{s}$, in Figure 4d, reflected waves can be observed at the top right of the snapshot which are propagating in a direction close to -135 deg . Those waves are reflected from the delamination damage of site #1.

From the SLDV scanning area, 10×10 points with the array spacing of 4 mm are selected to construct a rectangular grid array centered at the coordinate origin. Using the phased array imaging algorithms, an intensity image can be generated with the pixel definition given in Eq. (5). The resulting intensity image in Figure 5 clearly shows the presence of two delamination sites, represented as highlighted regions with site #1 at $(90.2, 42.8) \text{ mm}$ and site #2 at $(-10.4, 74.3) \text{ mm}$, where locations are based on the peak amplitude location. This detection result agrees well with the locations of actual delamination sites at $(88, 39) \text{ mm}$ and $(-11, 75) \text{ mm}$. The localization errors are less than 5 mm.

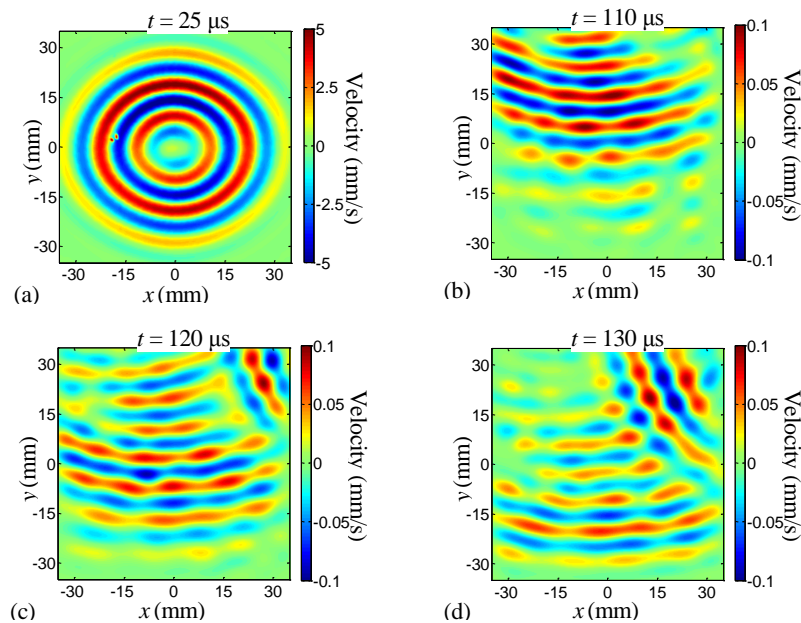


Figure 4 Snapshots of the wavefield measured by the SLDV:

(a) at $25 \mu\text{s}$, (a) at $110 \mu\text{s}$, (a) at $120 \mu\text{s}$, (a) at $130 \mu\text{s}$.

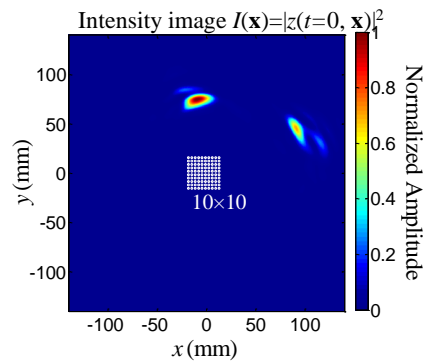


Figure 5 Phased array imaging result $I(x)$.

The 10×10 array used for phased array imaging is represented by the white dots.

CONCLUSIONS

This paper presents non-contact phased array approach for detecting multiple delaminations in composite plates. The phased array imaging algorithm is performed in frequency domain where both the guided wave dispersion effect and direction dependent wave properties are considered. Using the phased array imaging algorithm, an intensity image can be generated which clearly shows the damage location.

The presented phased array method is implemented with a non-contact SLDV system, which allows for the flexibility of using selected points from the SLDV scan to construct phased arrays of various configurations. The high spatial resolution of the SLDV system also significantly reduces array element spacing and allows the potential for using guided waves with smaller wavelengths to detect small defects in composite structures (compared to traditional phased array methods). Through a proof of concept experiment, this study shows that the non-contact phased array methods can detect two delaminations induced by impacts at different locations.

While the method presented here was successful at detecting two delaminations in a composite plate, further studies are still needed to improve the detection results. Besides the selected 120 kHz A_0 mode used in the current study, additional research needs to be performed with guided waves at other frequencies and/or different wave modes in highly anisotropic composite plates. The limitations of the technique in regards to the number of detectable damage sites and location of damage sites with respect to one another also needs further investigation.

ACKNOWLEDGEMENT

The authors would like to thank (1) the non-reimbursement space act umbrella agreement SAA1-18124 between South Carolina Research Foundation (SCRF) and the National Aeronautics and Space Administration (NASA) Langley Research Center, and (2) SC NASA EPSCoR Research Grant Program 521192-USCYu.

REFERENCES

- 1 Yu, L. and Giurgiutiu, V. (2008). "In Situ 2-D Piezoelectric Wafer Active Sensors Arrays for Guided Wave Damage Detection," *Ultrasonics*, 48(2), pp. 117-134.

- 2 Ambrozinski, L., Stepinski, T. and Uhl, T. (2014). "Efficient Tool for Designing 2D Phased Arrays in Lamb Waves Imaging of Isotropic Structures," *Journal of Intelligent Material Systems and Structures*, pp. online.
- 3 Wilcox, P. D. (2003). "Omni-directional guided wave transducer arrays for the rapid inspection of large areas of plate structures," *Ieee Transactions on Ultrasonics Ferroelectrics and Frequency Control*, 50(6), pp. 699-709.
- 4 Yan, F. and Rose, J. L. (2007). "Guided wave phased array beam steering in composite plates," *Health Monitoring of Structural and Biological Systems 2007*, 6532, pp. G5320-G5320.
- 5 Rajagopalan, J., Multila, K. H. M. O. A., Balasubramaniam, K. and Krishnamurthy, C. V. (2006). "A phase reconstruction algorithm for Lamb wave based structural health monitoring of anisotropic multilayered composite plates," *Journal of the Acoustical Society of America*, 119(2), pp. 872-878.
- 6 Vishnuvardhan, J., Muralidharan, A., Krishnamurthy, C. V. and Balasubramaniam, K. (2009). "Structural health monitoring of anisotropic plates using ultrasonic guided wave STMR array patches," *Ndt & E International*, 42(3), pp. 193-198.
- 7 Leleux, A., Micheau, P. and Castaings, M. (2013). "Long Range Detection of Defects in Composite Plates Using Lamb Waves Generated and Detected by Ultrasonic Phased Array Probes," *Journal of Nondestructive Evaluation*, 32(2), pp. 200-214.
- 8 Purekar, A. S. and Pines, D. J. (2010). "Damage Detection in Thin Composite Laminates Using Piezoelectric Phased Sensor Arrays and Guided Lamb Wave Interrogation," *Journal of Intelligent Material Systems and Structures*, 21, pp. 995-1010.
- 9 Wang, L. and Yuan, F. G. (2007). "Group Velocity and Characteristic Wave Curves of Lamb Waves in Composites: Modeling and Experiments," *Composites Science and Technology*, 67(7-8), pp. 1370-1384.
- 10 Glushkov, E., Glushkova, N. and Eremin, A. (2014). "Group velocity of cylindrical guided waves in anisotropic laminate composites," *Journal of Acoustic Society of America*, 135(1), pp. 148-154.
- 11 Nayfeh, A. H. (1995). *Wave propagation in layered anisotropic media*, Elsevier.
- 12 Yu, L. and Tian, Z. (2013). "Lamb Wave Structural Health Monitoring Using a Hybrid PZT-Laser Vibrometer Approach," *Structural Health Monitoring*, 12, pp. 469-483.
- 13 Yu, L., Tian, Z. and Leckey, C. A. C. (2015). "Crack imaging and quantification in aluminum plates with guided wave wavenumber analysis methods," *Ultrasonics*, 62, pp. 203-212.
- 14 Tian, Z. H., Yu, L. Y., Leckey, C. and Seebo, J. (2015). "Guided wave imaging for detection and evaluation of impact-induced delamination in composites," *Smart Materials and Structures*, 24(10), pp. 105019.
- 15 Tian, Z. and Yu, L. (2014). "Lamb Wave Frequency-Wavenumber Analysis and Decomposition," *Journal of Intelligent Material Systems and Structures*, 25(9), pp. 1107-1123.
- 16 Yu, L. Y. and Tian, Z. H. (2016). "Guided wave phased array beamforming and imaging in composite plates," *Ultrasonics*, 68, pp. 43-53.
- 17 Williams, G., Trask, R. and Bond, I. (2007). "A self-healing carbon fibre reinforced polymer for aerospace applications," *Composites Part a-Applied Science and Manufacturing*, 38(6), pp. 1525-1632.